

## EXPERIMENTS AND SIMULATIONS ON THE CLEANING OF A SWELLABLE SOIL IN PLANE CHANNEL FLOW

M. Joppa<sup>1</sup>, H. Köhler<sup>2</sup>, F. Rüdiger<sup>1</sup>, J.-P. Majschak<sup>2</sup> and J. Fröhlich<sup>1</sup>

<sup>1</sup> Institute of Fluid Mechanics, Technische Universität Dresden, 01062 Dresden, Germany, [matthias.joppa@tu-dresden.de](mailto:matthias.joppa@tu-dresden.de)

<sup>2</sup> Institute of Processing Machines and Mobile Machinery, Technische Universität Dresden, 01062 Dresden, Germany

### ABSTRACT

The cleaning behavior of a soil with physical properties that depend on the wetting time is studied experimentally via the local phosphorescence detection method and simulated numerically in fully developed plane channel flow for Reynolds numbers up to 30000. A computationally inexpensive general cleaning model is proposed adopting an existing removal model and coupling it to the turbulent flow field. The influence of the soil on the flow is neglected and the transient behavior of the soil during cleaning is modelled in form of a transient Dirichlet boundary condition. This approach is innovative for computational fluid dynamics of this phenomenon. The way of determining the model parameters from the experiment is described. The comparison of the simulation results with own experimental data reveals very good suitability of the model in case of a starch soil. A similar good agreement is found for data of a model protein foulant in tube flow from the literature.

### INTRODUCTION

It is indisputable that the cleaning in process plants, e.g. of heat exchangers, pipes or tanks, is an essential task in many industrial branches (Wilson, 2005). Environmental and economic constraints as well as stringent hygiene regulations, especially in the food industry, force companies to optimize the parameters of their automated cleaning in place (CIP) systems. Nonetheless those parameters nowadays are still determined empirically in most cases. A comprehensive review on cleaning in the food and beverage industry is given in Goode et al. (2013).

To overcome the drawback of empirically chosen parameters, the present authors target the prediction of the soil removal by means of Computational Fluid Dynamics (CFD), which is an innovation in the industrial context. Therefore, a computationally inexpensive CFD model for turbulent flow conditions is proposed which includes the removal model suggested by Xin et al. (2004) in form of a Dirichlet boundary condition to account for the soil behavior. A laboratory experiment is suggested to determine the soil dependent parameters of the model.

Here the validity of the model approach is assessed in two ways. First, the advantages of the implementation of the removal model in a CFD Solver are shown by simulating the pipe flow cleaning setup which was also used for validation purposes by Xin et al. (2004). In this case many of the removal parameters given there can be reused. Second, the laboratory experiment was carried out with a food-based swellable model soil. This configuration was recreated in the simulation, so that these results can directly be compared to the experimental data.

### EXPERIMENTAL TECHNIQUES

#### Soiling procedure

The model food soil used exemplarily in the laboratory experiment was a cold-soluble, pregelatinised waxy maize starch named 'C Gel – Instant 12410' which was produced by Cargill Deutschland GmbH. In a first step it had to be mixed with crystalline zinc sulfide which acts as a tracer in order to enable the use of the local phosphorescence detection method (LPD) described in Schöler et al. 2009. To this end, the tracer with a mean particle diameter of  $d = 2.8 \mu\text{m}$  was pre-mixed with distilled water at room temperature at a concentration of  $c = 4 \text{ g/l}$ . Afterwards the starch was dissolved in the suspension of tracer and distilled water at a concentration of  $c = 150 \text{ g/l}$  and a temperature of  $\vartheta = 23 \text{ }^\circ\text{C}$  while stirring with a frequency of  $f = 1200 \text{ rpm}$  for a time span of  $T = 30 \text{ min}$ .

In a second step the solution was applied to test sheets made of AISI 304 with a 2B finish, resulting in a surface roughness of  $R_z \leq 1 \mu\text{m}$ , on an area of  $A = (150 \times 80) \text{ mm}^2$ . Beforehand, these sheets were pre-cleaned with water, sonicated in an Elma S 30/H ultrasonic bath at a temperature of  $\vartheta = 30 \text{ }^\circ\text{C}$  for 10 min and wiped with ethanol. In the soiling process the sheets were placed horizontally and the test soil was sprayed on homogeneously.

During the last step, the sheets were dried at a constant temperature of  $\vartheta = 23 \text{ }^\circ\text{C}$  and a relative humidity of  $\phi = 50\%$  for a time span of  $T \approx 20 \text{ h}$ . The resulting soil layer is assumed to be smooth since the dry layer thickness was an order of magnitude larger than the tracer particle size on all test sheets.

**Test rig**

The cleaning experiments were performed in a closed loop cleaning test rig. It is schematically shown in Fig. 1. The rig was run with purified water acting as cleaning fluid at a temperature of  $\vartheta = (19.5 \pm 1) \text{ }^\circ\text{C}$ . Its measuring section is a channel with the cross sectional area of  $A = (78 \times 5) \text{ mm}^2$  and a bottom formed by a soiled test sheet. Optical accessibility is provided by a top wall made of Perspex. The supply channel and the drainage are designed to provide fully developed turbulent flow over the whole measuring section.

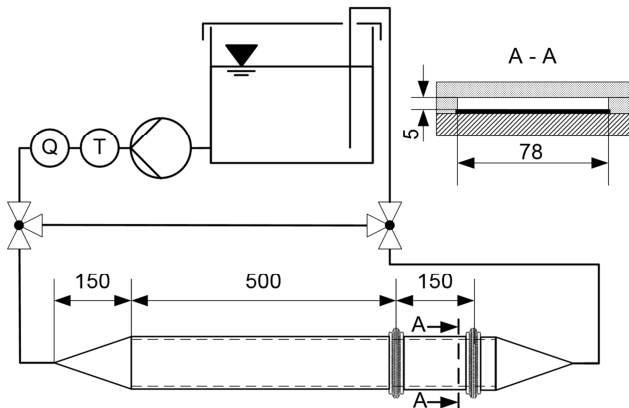


Fig. 1 Scheme of the cleaning test rig.

The test rig contains a bypass parallel to the measuring section allowing to reduce the startup delay which results from the acceleration of the cleaning fluid. Consequently, the cleaning process is initiated at a well-defined time. The experiment was controlled by a computer which regulated the volume flow rate to a defined mean bulk velocity. Two UVA lamps illuminated the fluorescent tracer within the soil. To maintain constant lighting conditions during cleaning the test section was surrounded by lightproof walls.

**Measuring procedure**

During the cleaning experiment, the change of fluorescence intensity of the soil was measured in situ using a camera (LPD) with a resolution of two megapixels and a monochrome grey scale resolution of fourteen bits. The resulting pictures were evaluated based on a centered zone with an area of  $A = (40 \times 40) \text{ mm}^2$ . The average grey scale value was determined within this region of interest. The resulting development of the grey scale value over time for two representative cases is shown in Fig. 2.

The curve representing the cleaning process at a bulk velocity of  $u_b = 1 \text{ m/s}$  shows that there is an initial increase of the grey scale value. Following the idea of the LPD, which presumes a linear relation between the grey scale value and the tracer concentration in the soil, this would represent an unreal increase of the amount of soil in the measuring area. The real reason of this effect becomes clear in comparison with an experiment performed at vanishing fluid velocity addressing the swelling behavior alone. It reveals that the increase of the grey scale value is

related to the swelling process. One reason could be the change of optical soil characteristics. This swelling influence on the grey scale value adds to the cleaning influence as it can be seen in the cleaning curve.

The elimination of the swelling influence to get a monotonically decreasing curve requires detailed knowledge concerning the removal and the swelling behavior and is therefore not trivial. That is why a simplified approach was chosen here. It is assumed that the soil removal starts at the maximum of the grey value curve, and the cleaning before the grey scale value peak is neglected. After the maximum the swelling influence is disregarded. Additionally, in order to quantitatively describe the soil removal, the grey value curve was scaled to start with the value of the initial surface soil coverage, termed  $m''_{s,0}$ . Examples of resulting curves are shown in Fig. 9 in the results section.

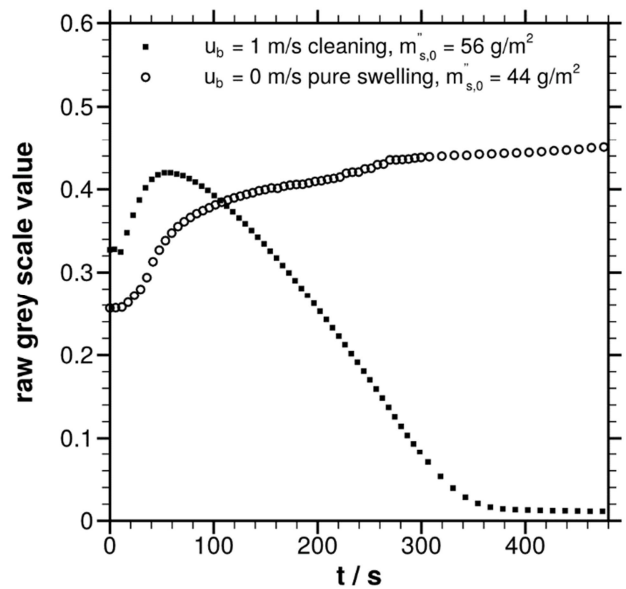


Fig. 2 Influence of the swelling process on the measured grey scale value: comparison of a pure swelling process (open symbols) and a case including soil removal (full symbols).

Altogether three different bulk velocities were used which resulted in Reynolds numbers up to  $Re = 30000$ . All relevant experimental parameters are summarized in Table 2. The reproducibility of the experimental results is illustrated in Fig. 3 for the example of  $Re = 10000$ . It reports the time  $t_{90}$  when 90 percent of the soil mass have been removed as a function of the initial surface soil coverage  $m''_{s,0}$ . Although substantial care has been taken to assure similar conditions in all runs, a large spreading cannot be denied. But this is typical for such experiments as shown in Fryer et al. (2011). Measures of the root mean square deviation  $\Delta_{rms}t_{90}$  and maximum deviation  $\Delta_{max}t_{90}$  are given in Table 3, normalized by the linear fit function of the experimental data providing  $t_{90} = f(m''_{s,0})$  for each flow configuration.

## COMPUTATIONAL METHODS

### Calculation of flow and mass transfer

The long-term goal of the present project is to develop a computational method to simulate the removal of a swellable soil in an industrial context. For physical reasons, and to make the problem tractable at reasonable effort, the following assumptions were made: First, the influence of the soil on the geometry of the flow is neglected, i.e. the flow geometry does not change upon soil removal, as this layer is comparatively thin. Second, the soil remains hydraulically smooth throughout the entire cleaning process. Third, the influence of the dissolved soil on the material parameters of the fluid is neglected. As a result of these assumptions flow and mass transfer decouple, so that a two-step procedure can be employed:

1. Calculate the mean flow field
2. Use the result to perform the mass transfer

One advantage of this approach is a strongly decreased calculation time compared to the fully coupled system. Furthermore, it is possible to use an experimentally measured flow field as basis for the second step.

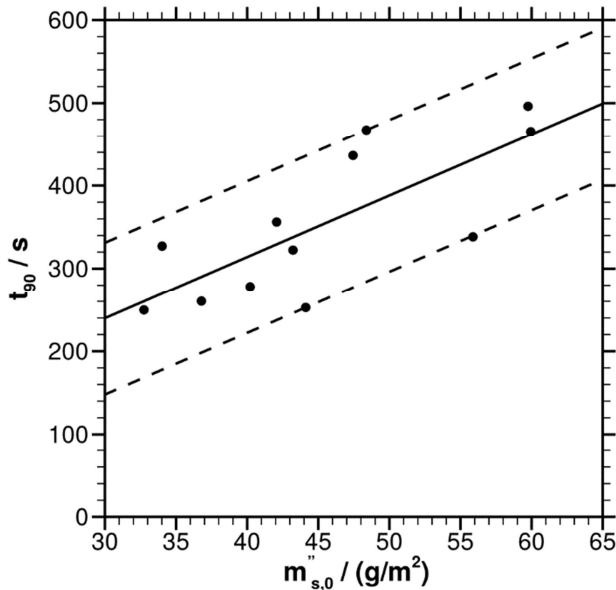


Fig. 3 Cleaning time in the experiments as a function of the initial surface soil coverage  $m''_{s,0}$  using the example of the time  $t_{90}$ , when 90 percent of the soil mass have been removed;  $Re = 10000$ ; the continuous line represents the linear fit function (coefficient of determination  $R^2 = 0.58$ ); the dashed lines represent the outer limits.

The fundamental equations of both steps were solved in the framework of OpenFOAM. In particular, the flow calculation was performed by solving the Reynolds averaged Navier Stokes equations (RANS) using the SST

turbulence model of Menter (1994). The turbulent viscosity  $\nu_t$  was evaluated in a way different from the standard OpenFOAM procedure by implementing a method similar to the one described in Fluent (2013). A Finite Volume method of second order was employed together with the PISO algorithm enhanced by outer loops and under-relaxation.

The convection-diffusion equation for the mean volume fraction of soil,  $\varphi$ , was solved with a Finite Volume method and central differences as well, employing an implicit time stepping of first order. A turbulent diffusion coefficient  $D_t$  was added to the molecular Diffusion Coefficient  $D$  and approximated as  $D_t = \nu_t / Sc_t$ . The turbulent Schmidt number was chosen to be  $Sc_t = 0.7$ . While the turbulent fluid velocity is statistically steady,  $\varphi$  is subjected to slowly varying unsteady boundary conditions described below. The convection-diffusion equation, hence, was modelled in unsteady RANS (URANS) fashion.

A scheme of the two-dimensional computational domain can be found in Fig. 4. It contains the coordinate system and the boundaries. The flow simulation features periodic conditions in streamwise direction, a no-slip-wall at the bottom and a symmetry boundary condition at the top boundary. The fully developed velocity field was obtained from a quasi-one-dimensional simulation.

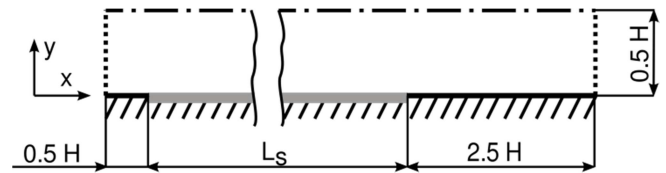


Fig. 4 Scheme of the computational domains including the main dimensions and the coordinate system;  $L_s$  denotes the initial length of the soil covered surface,  $H$  equals the channel height or the tube diameter.

When calculating the mass transfer and the soil removal homogeneous Neumann conditions are imposed for  $\varphi$  at the left, the right and the upper boundary. At the bottom wall a Dirichlet condition is imposed. At the soiled surface area of length  $L_s$ , the soil volume fraction  $\varphi$  is chosen as described in the following section. On the remaining part of the wall  $\varphi = 0$  is applied.

The mesh is constructed with increasing cell size in wall-normal direction. It is additionally local refined in the near-wall area resulting in a dimensionless wall distance of  $\Delta y_w^+ \approx 0.3$  in all simulations. The total number of mesh cells equals  $N = 33000$  in the channel geometry and  $N = 37000$  in the pipe geometry at the highest Reynolds number occurring.

### Modeling of the transient removal of a swelling soil

In the removal simulations carried out here the transient behavior of a swellable soil is included in terms of a transient Dirichlet boundary condition for the volume fraction of the soil  $\varphi$ . This condition is applied directly at the surface of the soil-covered wall. Hence the thickness

and the surface geometry of the soil layer are neglected. Figure 5 illustrates this approach which is innovative for CFD of the cleaning problem and adapted from the modelling of Xin et al. (2004).

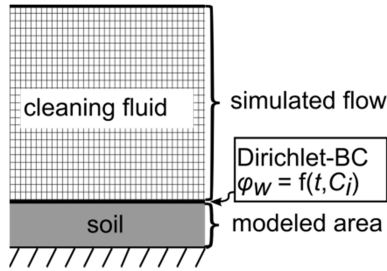


Fig. 5 Basic idea of the removal simulation: including the soil behavior in form of a transient Dirichlet boundary condition for the volume fraction of the soil in the cleaning fluid  $\varphi$ .

In that reference, an integral model for the removal of a swellable protein soil was proposed accounting for two cleaning stages: the swelling-uniform stage and the decay stage. Additionally the reptation time  $t_r$  is mentioned which elapses before the cleaning starts. With the present approach, an equivalent model is employed locally in form of a boundary condition. The resulting Dirichlet condition at the wall,  $\varphi = \varphi_w$ , reads

$$\varphi_w = \begin{cases} 0 & t < t_r \\ \varphi_{\max} \cdot e^{C_{sw}(t-t_r)} / (\Psi + e^{C_{sw}(t-t_r)}) & t \in [t_r, t_d] \\ \varphi_{\max} \cdot e^{-C_d(t-t_d)} & t > t_d \end{cases}, \quad (1)$$

where  $t_d$  identifies the start time of the decay stage while  $C_{sw}$ ,  $C_d$ ,  $\Psi$  and  $\varphi_{\max}$  denote other model parameters yet to be determined.

Given the computational setup described above, the removal rate  $\dot{m}_s''$  is calculated at each time step, locally for each cell of the soiled surface using Fick's law of diffusion

$$\dot{m}_s'' = -R (d\varphi/dy)_w. \quad (2)$$

It is therefore coupled to the flow field via the wall-normal derivative of the volume fraction at the soil-covered wall and the proportionality factor  $R$ . Contrary to the usual definition of  $R$  to be a diffusion coefficient, it is here interpreted as removal coefficient including diffusion itself and the cohesive removal of small pieces of soil.

In order to evaluate the cleaning progress, the remaining soil mass  $m_s''$  has to be determined. Therefore, an initial surface soil coverage  $m_{s,0}''$  is defined locally in each soil-covered boundary cell at the start of the simulation. This amount of soil is then reduced in every time step based

on the knowledge of the cleaning rate and the size of the time step. The simulation ends when the total remaining amount of soil falls below a threshold value.

The above equations contain several model parameters which have to be appropriately chosen in order to correctly predict the cleaning progress at any time. In particular, Eq. (1) holds six model parameters which define the behavior of a swellable soil:  $\varphi_{\max}$ ,  $t_r$ ,  $C_{sw}$ ,  $\Psi$ ,  $C_d$  and  $t_d$ . Furthermore, a suitable choice of the removal coefficient  $R$  and the diffusion coefficient  $D$  is necessary to calculate the removal rate in Eq. (2) and to achieve realistic diffusion behavior in the convection diffusion equation. Ideally, all these parameters should be soil-dependent but flow-independent constants. In that case the application of the cleaning model in other flow configurations would be straightforward and possible without any change of the parameters.

Hence, here some of the parameters are handled differently compared to Xin et al. (2004). First, the critical soil mass  $m_{s,t_d}'' = m_s''(t = t_d)$  is used instead of the decay time  $t_d$  to describe the beginning of the decay stage because  $m_{s,t_d}'' \neq f(Re)$  as stated by Xin et al (2004). Following this idea,  $t_d$  is set locally for each soil-covered boundary cell when the remaining mass in that cell falls below  $m_{s,t_d}''$ . Second, the decay parameter  $C_d$  is calculated from the critical soil mass  $m_{s,t_d}''$  and the removal rate at the beginning of the decay stage  $\dot{m}_{s,t_d}'' = \dot{m}_s''(t = t_d)$ . The appropriate relation can be derived by integrating Eq. (1) and following the commonly used concept of a mass transfer coefficient

$$\dot{m}_s'' = k(\varphi_w - \varphi_b) \quad (3)$$

where the volume fraction of soil in the bulk cleaning fluid  $\varphi_b$  is assumed to be negligible. The resulting model equation for the surface soil coverage  $m_s''$  reads

$$m_s'' = \begin{cases} m_{s,0}'' & t < t_r \\ m_{s,0}'' - \frac{\dot{m}_{s,\max}''}{C_{sw}} \cdot \ln\left(\frac{e^{C_{sw}(t-t_r)} + \Psi}{1 + \Psi}\right) & t \in [t_r, t_d] \\ \frac{\dot{m}_{s,\max}''}{C_d} \cdot e^{-C_d(t-t_d)} & t > t_d. \end{cases} \quad (4)$$

The evaluation of this equation at the time  $t_d$  in the decay stage yields the relation to calculate  $C_d$ . Written in a generalized form, the equation reads

$$C_d = \dot{m}_{s,t_d}'' / m_{s,t_d}'' \quad (5)$$

In the simulations, Eq. (5) is used immediately after the identification of the decay time and set locally for each soil-covered boundary cell. The third parameter adjustment

Table 1 Summary of parameters used to simulate the cleaning process of a model protein foulant in pipe flow on the basis of Xin et al. (2004);  $\nu = 4.7 \cdot 10^{-7} \text{ m}^2/\text{s}$ ,  $\rho = 980.6 \text{ kg/m}^3$ ,  $D = 8.71 \cdot 10^{-11} \text{ m}^2/\text{s}$ ,  $H = 16 \text{ mm}$ ,  $L_s/H = 9.375$ .

No.	$Re$	$m_{s,0}'' / (\text{g/m}^2)$	$t_r/\text{s}$	$R/(\text{g}/(\text{m s}))$	$C_{sw}/\text{s}^{-1}$	$\Psi$	$m_{s,t_d}''/(\text{g/m}^2)$	$C_d/\text{s}^{-1}$
1	3000	600	37.1	$6.81 \cdot 10^{-5}$	0.056	25	100	0.00681
2	8500	600	2.32	$6.81 \cdot 10^{-5}$	0.119	25	100	0.0122
3	15700	600	1.04	$6.81 \cdot 10^{-5}$	0.183	25	100	0.0181

targets the maximum volume fraction  $\varphi_{\max}$ . It is assumed to be  $\varphi_{\max} = 0.74$  which equals the fraction at the densest packing of spheres.

### Identification of removal model parameters

The coefficient  $R$  cannot be extracted from the simulation results and also cannot be estimated easily. In particular, it is calculated by using Eq. (2) in the plateau region at the end of the swelling stage via  $R = -\dot{m}_{s,\max}'' / (d\varphi/dy)_{w,\max}$ , where the term max denotes the temporal maximum. The maximum removal rate  $\dot{m}_{s,\max}''$  has to be extracted from experimental data. The maximum gradient of the soil volume fraction  $(d\varphi/dy)_{w,\max}$  can either be determined in an additional mass transfer simulation with a constant wall boundary condition of  $\varphi_w = \varphi_{\max}$  or it can be calculated by using an analytic correlation from the literature. Here, the first option was chosen. In both options the result is a decreasing gradient in downstream direction because of a growing concentration boundary layer. Therefore, the average gradient is determined in the soiled area.

The remaining parameters -  $\dot{m}_{s,\max}''$ ,  $t_r$ ,  $C_{sw}$ ,  $\Psi$  and  $m_{s,t_d}''$  - have to be identified by investigating experimental data. Here, two different sets of simulations were conducted, one for the configuration of Xin et al. (2004) and one in parallel to the own experiments. Consequently, two parameter sets were employed, depending on the configuration simulated. In Xin et al. (2004) the above five parameters are given for the tube configuration investigated and are hence employed as well in the simulations performed here. The calculation of the removal coefficient  $R$  in the way described above yields a constant value, which is a great finding because it is derived from two flow-dependent parameters. Hence, Eq. (2) seems to mirror the removal mechanism quite well. The resulting value was slightly corrected with one constant factor for all cases investigated in order to improve the agreement of the simulation results with the experimental values. This especially accounts for averaging issues coming along with the determination of  $R$ . All parameters employed in the present simulations are summarized in Table 1.

Appropriate parameters for the simulation of the plane channel configuration were extracted from the results of the laboratory experiment: The transient development of the surface soil coverage was directly measured by the LPD, so that the removal rate  $\dot{m}_s''(t)$  can be calculated via a differential quotient. Both are shown in Fig. 6 for one set of

flow conditions, together with appropriately parametrized model curves.

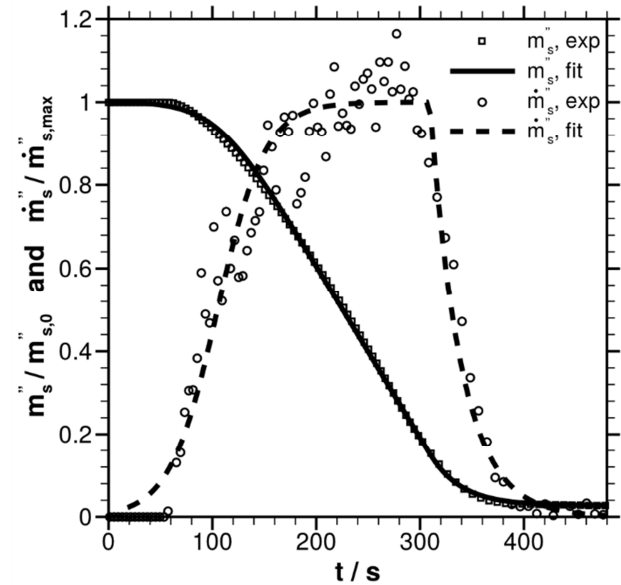


Fig. 6 Area averaged surface coverage  $m_s''$  and removal rate  $\dot{m}_s''$  in the present experiments for the case  $m_{s,0}'' = 56 \text{ g/m}^2$ ,  $Re = 10000$ . The fit curves show these quantities according to Eq. (4) and (1), respectively.

There are several options to determine the parameters. First, the parametrization procedure proposed by Xin et al. (2004) can be employed. Second, it is possible to use a least squares fit procedure to fit Eq. (1) to  $\dot{m}_{s,\text{exp}}''(t)$  because, following Eq. (3), the removal rate is proportional to the soil volume fraction at the wall. The third option is a least squares fit of Eq. (5) to  $m_{s,\text{exp}}''(t)$ . The fourth method considered here is the approach of the third option with some parameters -  $\Psi$ ,  $t_r$  and  $m_{s,t_d}''$  - fixed for all investigated flow conditions and chosen based on the results of the previously described options. This removes the Reynolds number dependency of these parameters which is advantageous for applications.

The quality of the described parameter determination methods is illustrated in Fig. 7 for the same flow conditions as in Fig. 6. These results are representative for all cases investigated.

Table 2 Summary of parameters used to simulate the cleaning process of a starch based soil in plane channel water flow;  $\nu = 9.35 \cdot 10^{-7} \text{ m}^2/\text{s}$ ,  $\rho = 997.54 \text{ kg/m}^3$ ,  $D = 10^{-11} \text{ m}^2/\text{s}$ ,  $H = 5 \text{ mm}$ ,  $L_s/H = 30$ .

No.	$Re$	$m_{s,0}'' / (\text{g/m}^2)$	$t_r/\text{s}$	$R/(\text{g}/(\text{m s}))$	$C_{sw}/\text{s}^{-1}$	$\Psi$	$m_{s,t_d}''/(\text{g/m}^2)$
1	10000	40	15	$2.5 \cdot 10^{-6}$	0.056	50	7.0
2	20000	40	15	$2.5 \cdot 10^{-6}$	0.119	50	7.0
3	30000	40	15	$2.5 \cdot 10^{-6}$	0.183	50	7.0
4	10000	50	15	$2.5 \cdot 10^{-6}$	0.056	50	7.0
5	10000	60	15	$2.5 \cdot 10^{-6}$	0.056	50	7.0

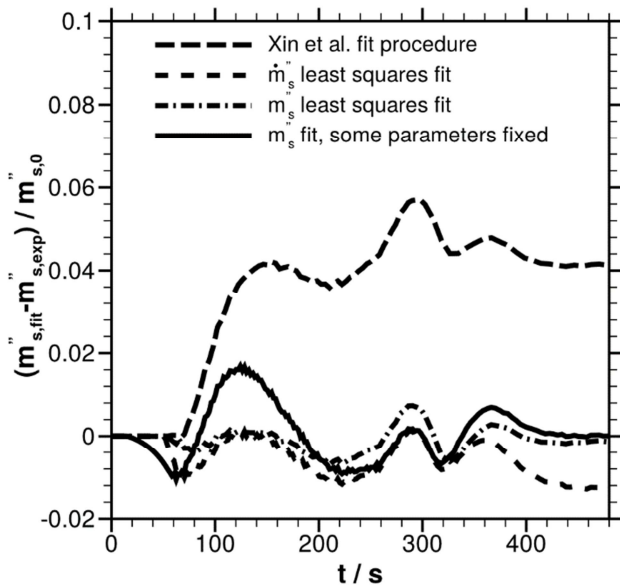


Fig. 7 Relative difference of the area averaged surface soil coverage  $m_s''$  between fit and experimental data for different approximation procedures as a function of the cleaning time  $t$  with  $m_{s,0}'' = 56 \text{ g/m}^2$  and  $Re = 10000$ . The legend entries correspond to the options one to four described in the text.

Obviously, the procedure proposed by Xin et al. (2004) yields the largest deviation although the relative difference is of acceptable size. The main problem with this method is the remaining offset at the end of the cleaning process, which leads to a large uncertainty of the determined total cleaning time. The same problem exists when the fit to the soil removal rate is performed. The best accuracy in determining the cleaning time is given by options three and four, or in other words with a fit to the curve of the remaining soil mass. Although the pure least squares fit shows a slightly lower deviation, option four is retained here because of the higher amount of flow-independent parameters. The final parameters are summarized in Table 2.

The removal coefficient  $R$  was calculated by using Eq. (2) as described above. It is to be mentioned that for the investigated flow conditions  $R$  showed an asymptotic behavior rather than a constant value. Nevertheless, the mean value was used. The other remaining flow-dependent parameter is  $C_{sw}$  which is linearly dependent on the Reynolds number and results from the fit.

## RESULTS AND DISCUSSION

### Cleaning simulation of a protein foulant in pipe flow

The purpose of this first set of simulations was to validate the present approach. To mimic the measuring method used by Xin et al. (2004), the removal rate in the simulation was determined by calculating the soil mass flux through the outlet boundary. Afterwards the latter was divided by the initially soiled surface area.

Figure 8 contains the transient removal rates  $\dot{m}_s''(t)$  of the simulation and the corresponding values of the experiment for three representative cases, differing by their Reynolds number. Bearing in mind the simplicity of the removal model and the typical scatter of experimental cleaning data the agreement is close to perfect. The locations of the global maxima as well as their size fit very well. Only the existence of local maxima right before the final decay in the higher Reynolds number cases is not included in the model equations.

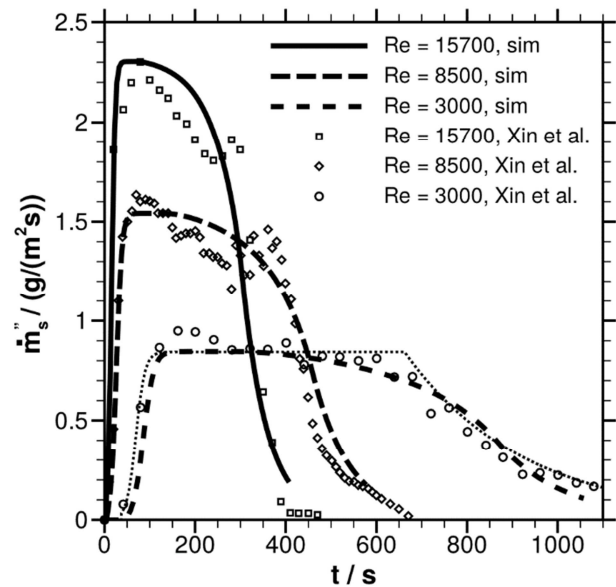


Fig. 8 Simulated area averaged cleaning rates  $\dot{m}_s''$  of a model protein foulant using the model parameters of Xin et al. (2004) in comparison with their experimental results. The dotted line represents  $\dot{m}_s''$  according to an integral use of Eq. (1) for one representative case.

As a result of the local use of Eq. (1) and its coupling to the flow, transient cleaning phenomena are taken into account: The concentration boundary layer causes large removal rates at the beginning of the soiled surface area. In downstream direction the removal rate decreases. Hence the local cleaning time varies as a function of the streamwise coordinate  $x$ . Consequently the transition between the cleaning stages in the averaged removal rate curves is appropriately reproduced. Non-natural bends of the curves between the cleaning stages which were existent in case of the integral use of the removal model equations in Xin et al. (2004) are avoided. This is illustrated in Fig. 8 for one representative case.

### Removal of a starch soil in plane channel flow

The second set of simulations was performed for the conditions of the own experiments using the parameters of Table 2. The validation of the results is done based on the transient development of the average remaining soil mass at the soil-covered boundary. Figure 9 contains the

experimental and computational results for three different Reynolds numbers and an initial surface soil coverage of  $m''_{s,0} \approx 40 \text{ g/m}^2$ .

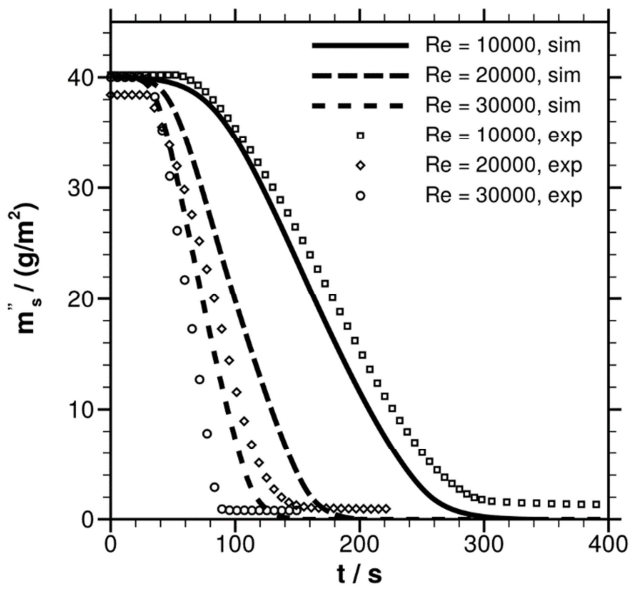


Fig. 9 Simulated area averaged surface soil coverage  $m''_s$  compared to own experimental data;  $m''_{s,0} \approx 40 \text{ g/m}^2$ .

The results show, as expected, a decreasing cleaning time with growing Reynolds numbers. The qualitative agreement between the experimental and the CFD results is very good. It is hence concluded that the removal model equations (1) are well suited to describe the cleaning process. The quantitative agreement is shown in Table 3, which contains the relative deviation between the simulation and the experiment regarding the cleaning time  $\Delta t_{90,sim}$ . This deviation is induced by the inappropriate choice of the removal coefficient  $R$ . As mentioned in the previous chapter, a constant value was assumed instead of taking the present asymptotic behavior into account. As a result the removal rates are overestimated for lower Reynolds numbers and underestimated for higher Reynolds numbers. Nevertheless, the deviations between the simulation and the experiment are similar to the experimental scatter range.

Another difference which has to be mentioned is the remaining soil in the experiment at the end of the cleaning process which is not present in the simulation. This

difference is caused by using Eq. (5) in the simulation which implies a complete cleaning of the surface. Actually a complete cleaning should be the case in an industrial cleaning process so that this is not a disadvantage of the approach.

Figure 10 illustrates the effect of the initial surface soil coverage on the cleaning process. In the simulations it is obvious that the results show an increasing total cleaning time in case of a growing initial soil mass. The sole model parameter which depends on this value is the starting time of the decay stage. Therefore the cleaning rate at the end of the swelling stage remains unchanged if the initial soil mass is sufficiently large. This effect is visible in Fig. 10 in terms of parallel curve progression. The experimental results do not clearly show this behavior because the measured cleaning rates are very sensitive to the initial conditions and soil geometry. Accordingly there is a large scatter in the cleaning time which was already discussed above and illustrated in Fig. 3.

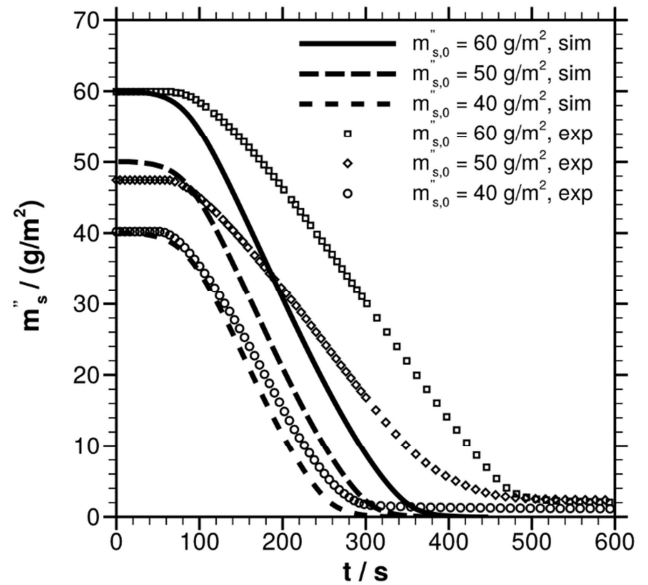


Fig. 10 Simulated area averaged surface soil coverage  $m''_s$  compared to own experimental data;  $Re = 10000$ .

Although the chosen cleaning coefficient  $R$  is afflicted with a systematical error as described above the deviation between the simulated and the measured values is in the range of the experimental scatter. This is true for all cases shown here. Nevertheless it is important to know that the

Table 3 Experimental scatter and the deviation between the simulation and the experiment regarding the cleaning time  $t_{90}$ . The reference values are calculated using the linear fit function of the experimental data providing  $t_{90} = f(m''_{s,0})$  for each flow configuration.

No.	$Re$	$m''_{s,0} / (\text{g/m}^2)$	$\Delta_{rms} t_{90,exp}$	$\Delta_{max} t_{90,exp}$	$\Delta t_{90,sim}$
1	10000	40	0.18	0.29	-0.23
2	20000	40	0.20	0.37	0.25
3	30000	40	0.14	0.23	0.36
4	10000	50	0.14	0.24	-0.28
5	10000	60	0.12	0.20	-0.31

influence of the cleaning coefficient on the cleaning time grows when the initial soil mass is increased so that the resulting uncertainty becomes important. Further attempts will be made to improve on this point.

## CONCLUSIONS

1. The paper proposes a CFD cleaning model which is able to reproduce the cleaning process of exemplary starch and protein foulants.
2. Compared to common CFD simulations of cleaning processes, the present approach is computationally inexpensive.
3. The implementation of the cleaning model can be adapted to another soil by determining five model parameters.
4. A laboratory experiment and a fit procedure were developed to provide access to the model parameters.
5. Just one of the parameters was found to be clearly flow-dependent. The others are soil-dependent constants.
6. The simulation of the cleaning process in configurations with different flow conditions, hence, may be possible by changing just one parameter.

## NOMENCLATURE

$A$	area, $m^2$
$C$	model parameter, $1/s$
$c$	concentration, $kg/m^3$
$D$	diffusion coefficient, $m^2/s$
$D_h$	hydraulic diameter, $D_h = 4A/P$ , $m$
$d$	diameter, $m$
$f$	stirring frequency, $1/s$
$H$	channel height or tube diameter, $m$
$k$	mass transfer coefficient, $kg/(m^2s)$
$L$	length, $m$
$m_s''$	surface soil coverage, $kg/m^2$
$\dot{m}_s''$	soil removal rate, $kg/(m^2s)$
$N$	number of elements, dimensionless
$P$	wetted perimeter, $m$
$R$	removal coefficient, $kg/(m\ s)$
$R^2$	coefficient of determination, dimensionless
$Re$	Reynolds number, $Re = u_b D_h / \nu$ , dimensionless
$R_z$	surface roughness defined by DIN EN ISO 4248, $m$
$Sc$	Schmidt number, $Sc = \nu / D$ , dimensionless
$T$	time span, $s$
$t$	time, $s$
$t_{90}$	time with ten percent of the initial soil remaining, $s$
$u$	velocity, $m/s$
$x$	axial coordinate, $m$
$y$	wall normal coordinate, $m$
$\Delta$	relative deviation, dimensionless
$\vartheta$	temperature, $^\circ C$
$\nu$	kinematic viscosity, $m^2/s$
$\rho$	density, $kg/m^3$
$\varphi$	volume fraction of soil, dimensionless
$\phi$	relative humidity, dimensionless

$\Psi$  model parameter, dimensionless

## Subscript

0	initial
b	bulk
d	decay
exp	experiment
max	maximum
r	reptation
rms	root mean square
s	soil
sim	simulation
sw	swelling
t	turbulent
w	wall

## REFERENCES

- Fluent Inc., 2013, *FLUENT 15 Theory Guide*, Southpointe, Canonsburg
- Fryer, P. J., Robbins, P. T., Cole, P. M., Goode, K. R., Zhang, Z., and Asteriadou, K., 2011, Populating the cleaning map: can data for cleaning be relevant across different lengthscales?, *Procedia Food Science*, Vol. 1, pp. 1761-1767.
- Goode, K. R., Asteriadou, K., Robbins, P. T., and Fryer, P. J., 2013, Fouling and cleaning studies in the food and beverage industry classified by cleaning type, *Comprehensive Reviews in Food Science and Food Safety*, Vol. 12, pp. 121-143.
- Menter, F. R., 1994, Two-Equation Eddy-Viscosity Turbulence Models for Engineering Applications, *AIAA Journal*, Vol. 32, pp. 1598-1605.
- Schöler, M., Fuchs, T., Helbig, M., Augustin, W., Scholl, S. and Majschak, J.-P., 2009, Monitoring of the local cleaning efficiency of pulsed flow cleaning procedures, *Proc. 8th Int. Conference on Heat Exchanger Fouling and Cleaning 2009*, Schladming, Austria, pp. 455-463.
- Wilson, D. I., 2005, Challenges in cleaning: recent developments and future prospects, *Heat Transfer Engineering*, Vol. 26, pp. 51-59.
- Xin, H., Chen, X. D., and Özkan, N., 2004, Removal of a model protein foulant from metal surfaces, *AIChE Journal*, Vol. 50, pp. 1961-1973.

## ACKNOWLEDGMENTS

This research project is supported by the Industrievereinigung für Lebensmitteltechnologie und Verpackung e.V. (IVLV), the Arbeitsgemeinschaft industrieller Forschungsvereinigungen 'Otto von Guericke' (AiF) and the Federal Ministry of Economic Affairs and Energy (AiF Project IGF 17805 BR).